Bol. Soc. Paran. Mat.
©SPM – E-ISSN-2175-1188
SPM: www.spm.uem.br/bspm

(3s.) **v. 2025 (43) 2** : 1–17.
ISSN-0037-8712
doi:10.5269/bspm.78991

A Leslie-Gower Model for Prey Harvesting with Predator Cooperation and Fear Responses

Mustak Euchuf, Ankur Jyoti Kashyap*, Anuradha Devi

ABSTRACT: This study proposes and analyzes a prey-predator harvesting model with a Michaelis-Menten type prey harvesting function. It incorporates the effects of fear induced by predation risk and predator hunting cooperation on prey growth. The model's biological feasibility is verified by ensuring the positivity and boundedness of its solutions. Equilibrium points are determined and their stability analyzed, with transcritical and saddle-node bifurcations examined using the Sotomayor approach. Numerical simulations show that increasing the catchability coefficient q or hunting cooperation rate α destabilizes the interior equilibrium, leading to prey-free states. Similarly, a decrease in the conversion coefficient b results in prey extinction. Key parameters affecting the emergence of prey-free states are also identified.

Key Words: Holling type II, Michaelis-Menten-type harvesting, fear effect, bifurcation analysis.

Contents

1. Introduction

Biodiversity on Earth is greatly influenced by complex ecological interactions, with predation playing a pivotal role in regulating species populations, shaping community structures, and driving evolutionary adaptations [4,5]. The classical theory of predation suggests that the primary influence of predators on prey populations stems from direct killing, with mortality viewed as the central mechanism shaping prey dynamics [6,7]. Recent studies have revealed that, in addition to direct killing, ecosystems are profoundly influenced by antipredator responses, such as fear-induced behaviors, which can alter prey distribution, behavior, and community dynamics. Prey species exhibit a variety of antipredator strategies, including changes in habitat use, foraging patterns, vigilance, and physiological responses. These adaptive behaviors can have lasting effects on the life history of prey, driving long-term morphological, behavioral, and physiological changes [8,9,10,11]. The impact of perceived predation risk on prey behavior has gained increasing attention in recent ecological research. A notable study by Zanette et al. [12] demonstrated that fear alone independent of actual predation led to a significant reduction of nearly 40% in the reproductive output of song sparrow parents. Based on their works, several models have explored predator-prey interactions where the fear of predation is critical in influencing prey growth and survival [11,13,14,2]. Among the various strategies employed by predators, cooperative hunting is a particularly influential tactic that intensifies fear among prey species. Predators often tailor their hunting strategies based on their nutritional needs; for instance, carnivores such as wolves, lions, and wild dogs frequently

* Corresponding author.
2010 *Mathematics Subject Classification:* 37N25, 34D23, 37M10, 37Gxx.
Submitted September 15, 2025. Published November 01, 2025

rely on group-based hunting to improve efficiency and success [15,16]. Similar cooperative behavior has also been observed in certain bird species, as well as arthropods like spiders and ants, which coordinate their efforts to enhance predation success. For such cooperation to be evolutionarily viable, the benefits to each participating individual must outweigh the physical effort invested in the hunt [17,18]. Cooperative hunting offers predators several advantages, such as reducing individual energy expenditure, while simultaneously exerting indirect effects on prey populations. One significant consequence for prey is a decline in fertility rates, which can, in turn, alter the demographic structure of entire ecosystems. For example, wolves are known to influence prey species such as elk not only through direct predation but also through the stress and fear induced by their cooperative hunting behavior [19,20]. In the presence of wolves, elk adopt various antipredator adaptations including changes in group size, habitat preference, vigilance, grazing behavior, and responsiveness to environmental cues to mitigate risk [21,22]. These sustained behavioral changes can culminate in chronic stress and reduced reproductive success, thereby reinforcing the ecological significance of fear as a non-consumptive effect of predation. Harvesting natural resources is a fundamental component of both ecological sustainability and economic management. From an ecological and socioeconomic perspective, it plays a crucial role in ensuring the long-term viability of biological resources. Harvesting strategies are commonly categorized into two main types: constant-yield harvesting, where a fixed quantity is removed regardless of population size, and constant-effort (or proportional) harvesting, where the harvested amount is proportional to the existing population density. Among these, constant-effort harvesting is frequently adopted in ecological modeling due to its analytical simplicity and practical relevance. However, traditional proportional harvesting models may not fully capture real-world constraints, particularly the saturation effects that emerge when stock density or harvesting effort becomes large. To address these limitations, researchers have proposed a Michaelis-Menten-type harvesting function, which introduces saturation dynamics similar to those observed in enzyme kinetics [23,24].

In this study, we propose a novel prey–predator interaction model that incorporates the combined effects of fear-induced responses and cooperative hunting behavior. Additionally, prey harvesting is modeled using a Michaelis-Menten-type functional response to reflect realistic saturation effects. The structure of the paper is as follows: Section 2 outlines the model formulation along with the underlying assumptions. Section 3 establishes the model's feasibility by proving the positivity and boundedness of its solutions. In Section 4, we analyze the biologically relevant equilibrium points and investigate their stability. Section 5 presents a bifurcation analysis centered on the interior equilibrium. Section 6 offers numerical simulations to support the analytical results, while Section 7 concludes with a discussion of the findings and their ecological implications.

2. Model formulation

Let us consider a Leslie–Gower prey–predator model, where $S(t)$ and $P(t)$ present the prey and predator biomass at any instant t. We assume the logistic growth rate of the prey to be r at any instant t with carrying capacity K, in the absence of predator P. The predator consumes the prey according to a Holling type II functional response and grows logistically with growth rate τ and carrying capacity $\frac{n_2+S}{b}$ proportional to the population size of the prey (or prey abundance). The parameter b is a measure of the food quantity that the prey provides and converted to predator birth. The term P/S is the Leslie–Gower term which measures the loss in the predator population due to rarity (per capita P/S) of its favorite food. Based on the preceding assumptions, the system's basic equations are Then we have the following model:

$$\begin{aligned} \frac{dS}{dt} &= rS\left(1-\frac{S}{k}\right)-\frac{aSP}{n_1+h_1S} \\ \frac{dP}{dt} &= \tau P\left(1-\frac{bP}{n_2+S}\right). \end{aligned} \tag{2.1}$$

Since fear due to predation risk indirectly reduces the reproduction rate, we modify (2.1) by multiplying the reproduction rate of the prey r by a factor $g(f,P)$ as follows:

$$\begin{aligned}\frac{dS}{dt} &= rS\left(1-\frac{S}{k}\right)g(f,P)-\frac{aSP}{n_1+h_1S}\\ \frac{dP}{dt} &= \tau P\left(1-\frac{bP}{n_2+S}\right)\end{aligned} \tag{2.2}$$

where P denotes predator biomass and parameter f depicts the intensity of fear which drives anti-predator behaviors of the prey. In biological aspects of f, P, $g(f,P)$, it is appropriate to assume:

$$\begin{aligned}&g(0,P)=1, g(f,0)=1, \lim_{f\to\infty} g(f,P)=0\\ &\lim_{P\to\infty} g(f,P)=0, \frac{\partial g(f,P)}{\partial f}<0, \frac{\partial g(f,P)}{\partial P}<0\end{aligned} \tag{2.3}$$

Here we consider $g(f,P)=(1+fP)^{-1}$ which satisfies condition (2.3). Then from system (2.2) we get,

$$\begin{aligned}\frac{dS}{dt} &= rS\left(1-\frac{S}{k}\right)\frac{1}{(1+fP)}-\frac{aSP}{n_1+h_1S}\\ \frac{dP}{dt} &= \tau P\left(1-\frac{bP}{n_2+S}\right).\end{aligned} \tag{2.4}$$

We assume that cooperative hunting provides a benefit to predators, leading to increased success in capturing prey as predator density rises. In recent years, considerable attention has been given to the phenomenon of cooperative hunting among predators [1]. Notably, Alves and Hilker [1] introduced predator-dependent functional responses to model this behavior, drawing from extensions of the classical Holling type II and type IV functional responses.

$$\begin{aligned}\phi_1(S,P) &= \frac{(a+\alpha P)SP}{1+h_1(a+\alpha P)S},\\ \phi_2(S,P) &= \frac{(a+\alpha P)SP}{1+h_2(a+\alpha P)S+h_3(a+\alpha P)S^2}.\end{aligned}$$

where h_1, h_2 represents handling time and h_3 represents how handling time increases with prey density due to group defence. a is the search rate of the predator towards the prey. We assume that the prey population does not possess the capacity to engage in group defence strategies against the predators. Furthermore, we generalize the functional response by incorporating n_1, which represents environmental protection to prey. Thus model (2.4) becomes:

$$\begin{aligned}\frac{dS}{dt} &= rS\left(1-\frac{S}{k}\right)\frac{1}{(1+f\alpha P)}-\frac{(a+\alpha P)SP}{(n_1+h_1S(a+\alpha P))},\\ \frac{dP}{dt} &= \tau P\left(1-\frac{bP}{n_2+S}\right).\end{aligned} \tag{2.5}$$

Next, non-linear harvesting is applied to the prey population following Michaelis–Menten type harvesting function

$$\mathbf{H}(S,\xi)=\frac{q\xi S}{m_1\xi+m_2S},$$

where q is the catchability coefficient of the species, ξ is the harvesting effort. The parameter m_1 is proportional to the ratio of the stock level to the harvesting rate (catch-rate) at higher levels of effort, and m_2 is proportional to the ratio of the effort level to the harvesting rate (catch-rate) at higher stock levels. With the above harvesting function, the system (2.5) becomes,

$$\begin{aligned}\frac{dS}{dt} &= rS\left(1-\frac{S}{k}\right)\frac{1}{(1+f\alpha P)}-\frac{(a+\alpha P)SP}{(n_1+h_1S(a+\alpha P))}-\frac{q\xi S}{m_1\xi+m_2S},\\ \frac{dP}{dt} &= \tau P\left(1-\frac{bP}{n_2+S}\right).\end{aligned} \tag{2.6}$$

subject to positive initial conditions $S(0) > 0$ and $P(0) > 0$.

3. Positivity and Boundedness

In this section, we have demonstrated the feasibility of the model (2.6) by verifying the positivity and boundedness of the solutions. Integrating Eq. (2.6) we get

$$\begin{aligned}
\int \frac{dS}{S} &= \int_0^t \left[r\left(1-\frac{S}{k}\right)\frac{1}{(1+f\alpha p)} - \frac{P(a+\alpha p)}{(n_1+h_1 S(a+\alpha P))} - \frac{qE}{m_1E+m_2S}\right]dt \\
\implies \Big[\log S\Big]_0^t &= \int_0^t \left[r\left(1-\frac{S}{k}\right)\frac{1}{(1+f\alpha P)} - \frac{p(a+\alpha p)}{(n_1+h_1 S(a+\alpha P))} - \frac{qE}{m_1E+m_2S}\right]dt \\
\implies log\left(\frac{S(t)}{S(0)}\right) &= \int_0^t \left[r\left(1-\frac{S}{k}\right)\frac{1}{(1+f\alpha p)} - \frac{(p(a+\alpha p)}{(n_1+h_1 S(a+\alpha P))} - \frac{qE}{m_1E+m_2S}\right]dt \\
\implies s(t) = s(0)\exp&\left[\int_0^t \left\{ rs(1-\frac{s}{k})\frac{1}{(1+f\alpha p)} - \frac{(sp(a+\alpha p)}{(n_1+h_1 S(a+\alpha P))} - \frac{qES}{m_1E+m_2S}\right\}\right]dt \qquad (3.1)
\end{aligned}$$

Similarly,

$$\begin{aligned}
\int \frac{dp}{P} &= \int_0^t \left\{\tau\left(1-\frac{bP}{n_2+S}\right)\right\}dt \\
\implies \Big[\log P\Big]_0^t &= \int_0^t \left\{\tau\left(1-\frac{bP}{n_2+S}\right)\right\}dt \\
\implies log\left(\frac{P(t)}{P(0)}\right) &= \int_0^t \tau\left(1-\frac{bP}{n_2+S}\right)dt \\
\implies P(t) = P(0)\exp&\left[\int_0^t \tau\left(1-\frac{bP}{n_2+S}\right)dt\right] \qquad (3.2)
\end{aligned}$$

From equations (3.1) and (3), it is clear that $S(t) \geq 0$ and $P(t) \geq 0$ whenever $S(0) > 0$ and $P(0) > 0$. Hence all solutions remain within the first quadrant of the xy-plane starting from an interior point of it. Further, we can easily establish that solution trajectories starting from $(S_0, 0)$ with $S_0 > 0$, remain within the positive x-axis at all future times and a similar result holds for trajectories starting from a point on the positive P-axis. Hence, $\mathbf{R}^2_+ = \{(S,P) : S, P \geq 0\}$ is an invariant set.

Boundedness: Consider $(S(t), P(t))$ be an arbitrary positive solution of the system (2.6) subject to a positive initial condition.Using the positivity of variables S, P and the first quation.of the system(2.6), we can write.

$$\begin{aligned}
\frac{dS}{dt} &= rS\left(1-\frac{S}{k}\right)\frac{1}{(1+f\alpha P)} - \frac{SP(a+\alpha P)}{(n_1+h_1 S(a+\alpha P))} - \frac{qES}{m_1E+m_2S} \\
&\leq rS\left(1-\frac{S}{k}\right)\frac{1}{(1+f\alpha P)} \leq rS\left(1-\frac{S}{k}\right) \\
\implies S(t) &\leq \max\{S(0), k\} = M_1, \quad \forall \ t \geq 0.
\end{aligned}$$

Now,

$$\begin{aligned}
S \leq M_1 &\implies n_2 + S \leq n_2 + M_1 \\
&\implies \frac{1}{n_2+S} \geq \frac{1}{n_2+M_1} \\
&\implies -\frac{1}{n_2+S} \leq -\frac{1}{n_2+M_1}
\end{aligned}$$

Therefore, from the second equation of the system (2.6), we have

$$\frac{dP}{dt} = \tau P\left(1 - \frac{bP}{n_2 + S}\right) \leq \tau P\left(1 - \frac{bP}{n_2 + M_1}\right)$$
$$\frac{dP}{dt} \leq \tau P\left(1 - \frac{P}{\frac{n_2+M_1}{b}}\right)$$

Therefore, $P(t) \leq \max\left\{P(0), \frac{n_2+M_1}{b}\right\} = M_2$, $\forall t \geq 0$. This completes the proof of the boundedness of solutions and hence the system under consideration is dissipative.

4. Equilibrium points

The system (2.6) has following trivial equilibrium points

1. Trivial or origin $E_0(0, 0)$.
2. Prey-free equilibrium $E_1\left(0, \frac{n_2}{b}\right)$, which always exists.
3. Predator-extinction equilibrium points are $E_L(S_L, 0)$ and $E_H(S_H, 0)$, where S_L and S_H are positive roots, the following quadratic equation
$$m_2 r S^3 + (m_1\xi r - k m_2 r)\, S^2 + (k\xi q - k m_1 \xi r)\, S = 0.$$
4. The interior equilibrium point $E^*(S^*, P^*)$ the points of intersection of the following two non-trivial nullclines,
$$\begin{aligned} \frac{b\tau P^2}{n_2 + S} - \tau P &= 0. \\ A_0 S P^3 + A_1 S P^2 + A_2 S P + S A_3 &= 0. \end{aligned} \tag{4.1}$$
where
$$\begin{aligned} A_0 &= \alpha^2 f k m_1 \xi + \alpha^2 f k m_2 S, \\ A_1 &= a\alpha f k m_1 \xi + a\alpha f k m_2 S + \alpha^2 f h_1 k \xi q S + \alpha k m_1 \xi + \alpha k m_2 S, \\ A_2 &= a\alpha f h_1 k \xi q S + a k m_1 \xi + a k m_2 S + \alpha f k \xi n_1 q - \alpha h_1 k m_2 r S^2 - \alpha h_1 k m_1 \xi r S \\ &\quad + \alpha h_1 k \xi q S + \alpha h_1 m_2 r S^3 + \alpha h_1 m_1 \xi r S^2, \\ A_3 &= -a h_1 k m_2 r S^2 - a h_1 k m_1 \xi r S + a h_1 k \xi q S + a h_1 m_2 r S^3 + a h_1 m_1 \xi r S^2 - k m_1 \xi n_1 r \\ &\quad - k m_2 n_1 r S + k \xi n_1 q + m_2 n_1 r S^2 + m_1 \xi n_1 r S. \end{aligned} \tag{4.2}$$

Local stability analysis:

In this section, we investigated the local stability of the feasible equilibrium points using Harmann-Grobman's theorem. Routh-Hurwitz theorem is utilised to discuss the local stability for those equilibrium points where the theoretical eigenvalues are hard to determine. The Jacobian matrix of the system (2.6) is given by

$$J = \begin{pmatrix} J_{11} & J_{12} \\ J_{21} & J_{22} \end{pmatrix} \tag{4.3}$$

where

$$\begin{aligned} J_{11} &= -\frac{n_1 P(a + \alpha P)}{(h_1 S(a + \alpha P) + n_1)^2} + \frac{r(k - 2S)}{\alpha f k P + k} - \frac{m_1 \xi^2 q}{(m_1\xi + m_2 S)^2}, \\ J_{12} &= S\left(\frac{\alpha f r(S - k)}{k(\alpha f P + 1)^2} - \frac{h_1 S(a + \alpha P)^2 + n_1(a + 2\alpha P)}{(h_1 S(a + \alpha P) + n_1)^2}\right), \\ J_{21} &= \frac{bP^2\tau}{(n_2 + S)^2}, J_{22} = \tau - \frac{2bP\tau}{n_2 + S}. \end{aligned}$$

(i) At the trivial equilibrium E_0, the Jacobian matrix (4.3) has the eigenvalues $\lambda_{01} = \tau$, and $\lambda_{02} = \frac{m_1 r - q}{m_1}$. Since one of the eigenvalues is non-negative, therefore E_0 is always unstable. If $\lambda_{02} < 0$,i.e., if $m_1 r < q$, the trivial equilibrium E_0 is a saddle point.

(ii) At the prey-free equilibrium E_1, the Jacobian matrix (4.3) has the eigenvalues $\lambda_{11} = -\tau$ and $\lambda_{12} = -\frac{n_2(ab+\alpha n_2)}{b^2 n_1} + \frac{br}{b+\alpha f n_2} - \frac{q}{m_1}$. Therefore, E_1 is locally asymptotically stable if $\lambda_{12} < 0$, i.e., $\frac{br}{b+\alpha f n_2} < \frac{n_2(ab+\alpha n_2)}{b^2 n_1} + \frac{q}{m_1}$.

(iii) At the predator-free equilibra E_L and E_H, the Jacobian matrix (4.3) has the eigenvalues $\lambda_{21} = \tau$ and $\lambda_{22} = -\frac{2rS_L}{k} - \frac{m_1 \xi^2 q}{(m_2 S_L + m_1 \xi)^2} + r$. Since one of the eigenvalues is non-negative, therefore E_L is always unstable. Similarly, E_H is always unstable.

(iv) To study the behaviour of the system near the interior equilibrium E^*, we utilise the Routh-Hurwitz theorem. Because of the complexity of the model, the calculation of theoretical eigenvalues is not possible. The characteristic equation of the Jacobian matrix (4.3) at $E^*(S^*, P^*)$ is given by

$$X^2 - A_1(S^*, P^*)X + A_2(S^*, P^*) = 0 \tag{4.4}$$

The above characteristic equation will have at least one zero with a positive real part if (a) $A_2 < 0$ or (b) $A_2 > 0$ and $A_2 > 0$. Thus the equilibrium state E^* is unstable under these conditions. On the other hand, if $A_2 > 0$, $A_1 < 0$, then both the zeros of the characteristic equation of the Jacobian matrix (4.3) are negative or have a negative real part, and hence the equilibrium state is locally asymptotically stable.

5. Bifurcation analysis

Theorem 5.1 *At the critical parameter $b = b^{BP}$, the system (2.6) at the prey-free equilibrium E_1 undergoes a transcritical bifurcation if*

$$v_1 \left(\frac{2h_1 n_2 \left(ab^{BP} + \alpha n_2\right)^2}{(b^{BP})^3 n_1^2} + \frac{2m_2 q}{m_1^2 \xi} - \frac{2b^{BP} r}{bk + \alpha f k n_2} \right) - \frac{v_2}{b^{BP}} \left(\frac{ab^{BP} + 2\alpha n_2}{n_1} + \frac{\alpha (b^{BP})^3 f r}{\left(b^{BP} + \alpha f n_2\right)^2} \right) \neq 0,$$

where b^{BP} is the positive root of the equation

$$b^3 \left(n_1 q - m_1 n_1 r\right) + b^2 \left(a m_1 n_2 + \alpha f n_1 n_2 q\right) + b \left(a \alpha f m_1 n_2^2 + \alpha m_1 n_2^2\right) + \alpha^2 f m_1 n_2^3 = 0.$$

Proof:

The Jacobian matrix of the system (2.6) at the prey-free equilibrium E_1 has an eigenvalue zero at the critical parameter $b = b^{BP}$. So the eigenvalue analysis method fails to predict the nature of the equilibrium point at the critical value b^{BP}. Therefore we use Sotomayor's theorem [3] to investigate the nature of the equilibrium E_1 at $b = b^{BP}$. Rewrite the system (2.6) as follows:

$$\frac{dX}{dt} = g(X, b) = [g_1(X, b), g_2(X, b)]^T,$$

where $X = \begin{pmatrix} S \\ P \end{pmatrix}$, $g_1(X, b) = \frac{dS}{dt}$, and $g_2(X, b) = \frac{dP}{dt}$.

The eigenvectors of J_{E_1} and $[J_{E_1}]^T$ corresponding to the zero eigenvalue at $b = b^{BP}$ are $V = [v_1, v_2]^T$ and $W = [w_1, w_2]^T$ Then we have

$$W^T g_b(X, b^{BP})_{E_1} = 0,$$

$$W^T D g_b(X, b^{BP})(V)_{E_1} \frac{\tau w_2 \left(v_1 - 2b^{BP} v_2\right)}{(b^{BP})^2} \neq 0.$$

Therefore, the first two conditions of the transcritical bifurcation are met while saddle-node and pitchfork bifurcation cannot occur. Now

$$W^T D^2 g(X, b^{BP})(V,V)_{E_1}$$
$$= v_1 \left(\frac{2h_1 n_2 \left(ab^{BP} + \alpha n_2\right)^2}{(b^{BP})^3 n_1^2} + \frac{2m_2 q}{m_1^2 \xi} - \frac{2b^{BP} r}{bk + \alpha f k n_2} \right) - \frac{v_2}{b^{BP}} \left(\frac{ab^{BP} + 2\alpha n_2}{n_1} + \frac{\alpha (b^{BP})^3 fr}{(b^{BP} + \alpha f n_2)^2} \right)$$
$$\neq 0.$$

Thus the system satisfies all the conditions of Sotomayor's theorem for transcritical bifurcation. Therefore the system (2.6) undergoes a transcritical bifurcation at the parameter $b = b^{BP}$ at the predator-free equilibrium E_1.

□

Theorem 5.2 *At the critical parameter $q = q^{BP} = m_1 \left(\frac{br}{b+\alpha f n_2} - \frac{n_2(ab+\alpha n_2)}{b^2 n_1} \right)$, the system (2.6) at the prey-free equilibrium E_1 undergoes a transcritical bifurcation if*

$$w_1 \left[v_1 \left(\frac{2h_1 n_2 \left(ab + \alpha n_2\right)^2}{b^3 n_1^2} - \frac{2m_2}{m_1 \xi} \left(\frac{n_2 \left(ab + \alpha n_2\right)}{b^2 n_1} - \frac{br}{b + \alpha f n_2} \right) - \frac{2br}{bk + \alpha f k n_2} \right) \right.$$
$$\left. + \frac{v_2 \left(-\frac{ab+2\alpha n_2}{n_1} - \frac{\alpha b^3 fr}{(b+\alpha f n_2)^2} \right)}{b} \right] + \frac{2\tau w_2 \left(v_1 - b v_2\right)}{n_2} \neq 0.$$

Proof:

The Jacobian matrix of the system (2.6) at the prey-free equilibrium E_1 has an eigenvalue zero at the critical parameter $q = q^{BP}$. So the eigenvalue analysis method fails to predict the nature of the equilibrium point at the critical value q^{BP}. Therefore we use Sotomayor's theorem [3] to investigate the nature of the equilibrium E_1 at $q = q^{BP}$. Rewrite the system (2.6) as follows:

$$\frac{dX}{dt} = g(X, q) = [g_1(X, q), g_2(X, q)]^T,$$

where $X = \begin{pmatrix} S \\ P \end{pmatrix}$, $g_1(X, q) = \frac{dS}{dt}$, and $g_2(X, q) = \frac{dP}{dt}$.

The eigenvectors of J_{E_1} and $[J_{E_1}]^T$ corresponding to the zero eigenvalue at $q = q^{BP}$ are $V = [v_1, v_2]^T$ and $W = [w_1, w_2]^T$ Then we have

$$W^T g_q(X, q^{BP})_{E_1} = 0,$$
$$W^T D g_q(X, q^{BP})(V)_{E_1} = -\frac{v_1 w_1}{m_1} \neq 0.$$

Therefore, the first two conditions of the transcritical bifurcation are met while saddle-node and pitchfork bifurcation cannot occur. Now

$$W^T D^2 g(X, q^{BP})(V,V)_{E_1} =$$
$$w_1 \left[v_1 \left(\frac{2h_1 n_2 \left(ab + \alpha n_2\right)^2}{b^3 n_1^2} - \frac{2m_2}{m_1 \xi} \left(\frac{n_2 \left(ab + \alpha n_2\right)}{b^2 n_1} - \frac{br}{b + \alpha f n_2} \right) - \frac{2br}{bk + \alpha f k n_2} \right) \right.$$
$$\left. + \frac{v_2}{b} \left(-\frac{ab + 2\alpha n_2}{n_1} - \frac{\alpha b^3 fr}{(b + \alpha f n_2)^2} \right) \right] + \frac{2\tau w_2 \left(v_1 - b v_2\right)}{n_2} \neq 0.$$

Thus the system satisfies all the conditions of Sotomayor's theorem for transcritical bifurcation. Therefore the system (2.6) undergoes a transcritical bifurcation at the parameter $q = q^{BP}$ at the predator-free equilibrium E_1.

□

Theorem 5.3 *At the critical parameter $\alpha = \alpha^{BP}$, the system (2.6) at the prey-free equilibrium E_1 undergoes a transcritical bifurcation if*

$$w_1\left[v_1\left(\frac{2h_1n_2\left(ab+\alpha^{BP}n_2\right)^2}{b^3n_1^2}-\frac{2m_2}{m_1\xi}\left(\frac{n_2\left(ab+\alpha n_2\right)}{b^2n_1}-\frac{br}{b+\alpha^{BP}fn_2}\right)-\frac{2br}{bk+\alpha^{BP}fkn_2}\right)\right.$$
$$\left.+\frac{v_2}{b}\left(-\frac{ab+2\alpha^{BP}n_2}{n_1}-\frac{\alpha^{BP}b^3fr}{\left(b+\alpha^{BP}fn_2\right)^2}\right)\right]+\frac{2\tau w_2\left(v_1-bv_2\right)}{n_2}\neq 0.$$

where α^{BP} is the positive root of the equation

$$fm_1n_2^3\alpha^2+\alpha\left(abfm_1n_2^2+b^2fn_1n_2q+bm_1n_2^2\right)+\left(ab^2m_1n_2-b^3m_1n_1r+b^3n_1q\right)=0.$$

Proof:

The Jacobian matrix of the system (2.6) at the prey-free equilibrium E_1 has an eigenvalue zero at the critical parameter $\alpha = \alpha^{BP}$. So the eigenvalue analysis method fails to predict the nature of the equilibrium point at the critical value α^{BP}. Therefore we use Sotomayor's theorem [3] to investigate the nature of the equilibrium E_1 at $\alpha = \alpha^{BP}$. Rewrite the system (2.6) as follows:

$$\frac{dX}{dt}=g(X,\alpha)=[g_1(X,\alpha),g_2(X,\alpha)]^T,$$

where $X=\begin{pmatrix}S\\P\end{pmatrix}$, $g_1(X,\alpha)=\frac{dS}{dt}$, *and* $g_2(X,\alpha)=\frac{dP}{dt}$.

The eigenvectors of J_{E_1} and $[J_{E_1}]^T$ corresponding to the zero eigenvalue at $\alpha = \alpha^{BP}$ are $V=[v_1,v_2]^T$ and $W=[w_1,w_2]^T$ Then we have

$$W^Tg_\alpha(X,\alpha^{BP})_{E_1}=0,$$
$$W^TDg_\alpha(X,\alpha^{BP})(V)_{E_1}=v_1w_1\left(-\frac{n_2^2}{b^2n_1}-\frac{bfn_2r}{\left(b+fn_2\alpha^{BP}\right)^2}\right)\neq 0.$$

Therefore, the first two conditions of the transcritical bifurcation are met while saddle-node and pitchfork bifurcation cannot occur. Now

$$W^TD^2g(X,\alpha^{BP})(V,V)_{E_1}$$
$$w_1\left[v_1\left(\frac{2h_1n_2\left(ab+\alpha^{BP}n_2\right)^2}{b^3n_1^2}-\frac{2m_2}{m_1\xi}\left(\frac{n_2\left(ab+\alpha n_2\right)}{b^2n_1}-\frac{br}{b+\alpha^{BP}fn_2}\right)-\frac{2br}{bk+\alpha^{BP}fkn_2}\right)\right.$$
$$\left.+\frac{v_2}{b}\left(-\frac{ab+2\alpha^{BP}n_2}{n_1}-\frac{\alpha^{BP}b^3fr}{\left(b+\alpha^{BP}fn_2\right)^2}\right)\right]+\frac{2\tau w_2\left(v_1-bv_2\right)}{n_2}\neq 0.$$

Thus the system satisfies all the conditions of Sotomayor's theorem for transcritical bifurcation. Therefore the system (2.6) undergoes a transcritical bifurcation at the parameter $\alpha = \alpha^{BP}$ at the predator-free equilibrium E_1.

□

Theorem 5.4 The interior equilibrium state E^* of the system encounters saddle-node bifurcation with respect to the parameter α under the following condition,

$$w_1\left(v_1\chi_{11}+v_2\chi_{12}\right)+w_2\left(v_1\chi_{21}+v_2\chi_{22}\right)\neq 0,$$

where $\chi_{ij}, i,j=1,2$, are defined within the proof.

Proof: *The Jacobian of the system (2.6) around the interior equilibrium state E^* has an eigenvalue equal to zero at the critical parameter q^{LP}. Due to the occurrence of zero eigenvalue, the eigen analysis*

method fails to predict the nature of the equilibrium state at the critical value q^{LP}. *Therefore we use Sotomayor's theorem [3] to investigate the nature of the equilibrium* E^* *at the* q^{LP}. *Rewrite the system (2.6) as follows:*

$$\frac{dX}{dt} = \hat{h}(X,\alpha) = [\hat{h}_1(X,q), \hat{h}_2(X,q)]^T,$$

where $X = \begin{pmatrix} S \\ P \end{pmatrix}$, $\hat{h}_1(X,q) = \frac{dS}{dt}$ *and* $\hat{h}_2(X,q) = \frac{dP}{dt}$.
Let $V = [v_1, v_2]^T$ *and* $W = [w_1, w_2]^T$ *are respectively the eigenvectors of* J_{E^*} *and* $[J_{E^*}]^T$ *corresponding to the zero eigenvalue at* $q = q^{LP}$.
Here,

$$D^2\hat{h}(X, q^{LP})(V,V)_{E^*} = \begin{pmatrix} v_1\chi_{11} + v_2\chi_{12} \\ v_1\chi_{21} + v_2\chi_{22} \end{pmatrix},$$

where

$$\begin{aligned}
\chi_{11} &= \frac{h_1 n_1 P^* \left(a + \alpha P^*\right)^2}{\left(h_1 S^* \left(a + \alpha P^*\right) + n_1\right)^3} - \frac{r}{\alpha f k P^* + k} + \frac{m_1 m_2 \xi^2 q}{\left(m_1\xi + m_2 S^*\right)^3}, \\
\chi_{12} &= -\frac{n_1\left(a h_1 S^*\left(a + \alpha P^*\right) + n_1\left(a + 2\alpha P^*\right)\right)}{\left(h_1 S^*\left(a + \alpha P^*\right) + n_1\right)^3} - \frac{\alpha f r\left(k - 2S^*\right)}{k\left(\alpha f P^* + 1\right)^2}, \\
\chi_{21} &= \frac{2b\tau P^*}{\left(n_2 + S^*\right)^2}, \\
\chi_{22} &= -\frac{2b\tau}{n_2 + S^*}.
\end{aligned}$$

Now,

$$\begin{aligned}
W^T \hat{h}_\alpha(X, q^{BP})_{E^*} &= 0, \\
W^T D^2\hat{h}(X, q^{BP})(V,V)_{E^*} &\neq 0,
\end{aligned}$$

if $w_1\left(v_1\chi_{11} + v_2\chi_{12}\right) + w_2\left(v_1\chi_{21} + v_2\chi_{22}\right) \neq 0$. *Thus, the system satisfies all Sotomayor's theorem's saddle-node bifurcation conditions. Therefore the system (2.6) undergoes saddle-node bifurcation near the interior equilibrium* E^* *at the parameter* $q = q^{BP}$. □

6. Computational results

In this section, we conduct numerical simulations using a biologically plausible set of parameters mentioned in Table 1. We consider the initial population of the ecosystem to be $S = 10$ and $P = 15$. For the parameters mentioned in Table 1, there exist four different equilibria E_0, E_1, E_H and E^*. The interior equilibrium point plays a significant role in the study of ecosystems. In an ecological sense, a stable interior equilibrium indicates a stable population of species within the ecosystem over a certain period of time. Due to different biotic or abiotic factors, populations of species within an ecosystem often get disturbed, and the equilibrium state becomes unstable. For the above initial conditions, the trajectories of the system approach to $E^*(2.96, 7.93)$ (Figure 1, 2). From Figure 2, it is clear that the interior equilibrium E^* may have a large basin of attraction.

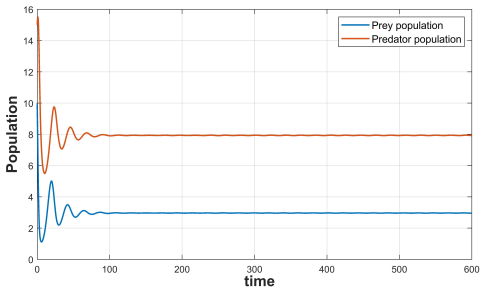

Figure 1: Time series of the system (2.6) for parameters in Table 1.

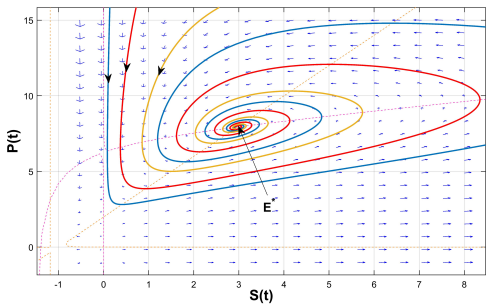

Figure 2: Phase Portrait of the system (2.6) for parameters in Table 1.

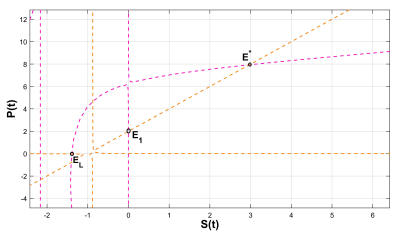

(a)

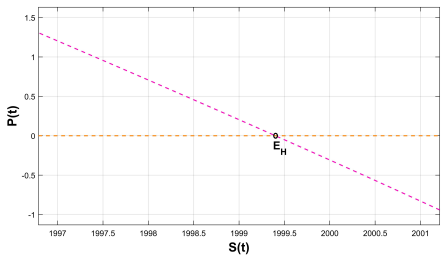

(b)

Figure 3: The equilibrium states of the system (2.6) for of the parameter $f = 0$ and $q = 0.9$ (keeping other parameter values as listed in Table 1).

Description	Parameter	Default value
Reproduction rate of prey	r	0.5
Carrying capacity	k	2000
Strength of fear	f	0.2
Predation rate	a	0.2
Environmental protection to prey	n_1	10
Catchability coefficient	q	0.03
Harvesting effort	ξ	1
Proportionality constant	m_1	0.2
Proportionality constant	m_2	0.1
Growth rate of predator	τ	0.1
Conversion coefficient	b	0.5
Environmental protection to predator	n_2	1
Hunting cooperation rate	α	0.05
Handling time	h_1	1

Table 1: Parameters. Units are considered in *per unit time*.

Type	**Bifurcation point**	**State space**	**Lyapunov coefficient**
Hopf	$b^H = 1.097356$	$(10.370064, 10.361327)$	$l_1 = 2.534477 \times 10^{-04}$
Hopf	$\tau^H = 0.095872$	$(2.966605, 7.933209)$	$l_1 = 9.745807 \times 10^{-04}$
Transcritical	$b^{BP} = 0.159919$	$(0, 6.253171)$	
Transcritical	$q^{BP} = 0.086039$	$(0, 6.253171)$	
Transcritical	$\alpha^{BP} = 0.549693$	$(0, 2)$	
Saddle-Node	$q^{LP} = 0.098112$	$(0.916280, 3.832559)$	
GH	$(\tau = 2.792823, f = 0.049492)$	$(1.484081, 4.968162)$	
GH	$(\tau = 0.071546, q = 0.119494)$	$(2.204269, 6.408538)$	
GH	$(\tau = 1.963376, r = 1.039781)$	$(13.627614, 29.255228)$	
GH	$(f = 1.086663, b = 2.307382)$	$(24.942309, 11.243181)$	
GH	$(\alpha = 1.266175, b = 2.726527)$	$(5.341842, 2.325978)$	
GH	$(q = 0.148650, b = 0.884325)$	$(3.803422, 5.431738)$	
BT	$(\tau = 0.098112, q = 0.110503)$	$(0.916279, 3.832558)$	

Table 2: Bifurcation points obtained numerically.

We initiate from the interior equilibrium point E^* and keep the conversion coefficient (b) as a free variable. On increasing b, we observe that the E^* becomes unstable through a Hopf bifurcation at $b^H = 1.097356$ with state space $(10.370064, 10.361327)$. The nature of the Hopf bifurcation is subcritical with first Lyapunov coefficient $l_1 = 2.534477 \times 10^{-04}$. At this threshold point, one of the eigenvalues of the Jacobian matrix at E^* becomes 0 and both the population starts oscillating periodically for $b > b^H$. Figure 4 depicts the time series solution and phase portrait of the system for $b = 1.2$ and other parameters as in Table 1. Again, we consider τ to be a free parameter and initiate from the interior equilibrium E^*. On decreasing τ, the interior equilibrium E^* becomes unstable through a Hopf bifurcation at $\tau^H = 0.095872$ with state space $(2.966605, 7.933209)$. Below this threshold parameter τ^H, both populations start oscillation periodically. The nature of the Hopf bifurcation is subcritical with first Lyapunov coefficient $l_1 = 9.745807 \times 10^{-04}$. Figure 5 depicts the time series solution of the system for $\tau = 0.05$ and other parameters as in Table 1.

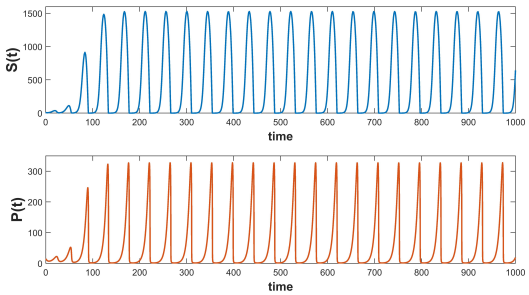

(a)

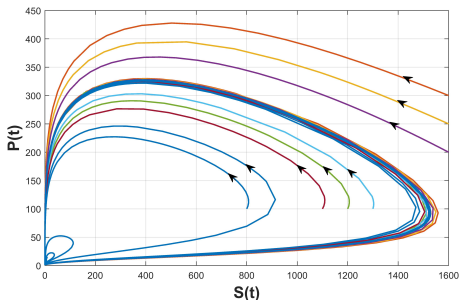

(b)

Figure 4: Time series and Phase portrait for $b = 1.2$.

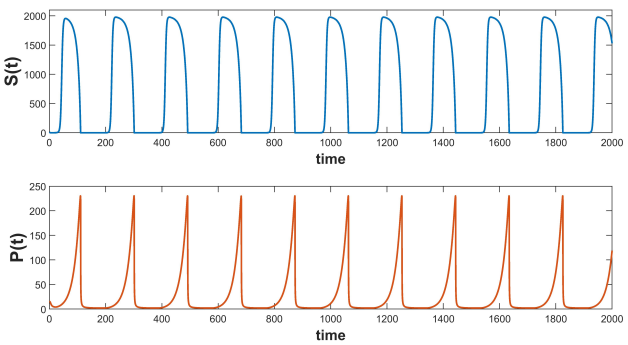

Figure 5: Time series for $\tau = 0.05$

Next, we start from the Hopf bifurcation point $\tau = \tau^H$, and plot two dimensional projection of Hopf bifurcation curves in the parameter spaces (f, τ),(q, τ) and (r, τ) (Figure 6). It is observed that in all cases, the Hopf curves lead to the detection of Generalised-Hopf bifurcation points, where the nature of the Hopf bifurcation changes from subcritical to supercritical. The plotted Hopf curves in Figure 6, separate each region into two parts where the interior equilibrium shows two different natures; stable and unstable. In unstable regions, both populations of the ecosystem show oscillatory behaviour, resulting in an unstable interior equilibrium. Similar Hopf curves are plotted in Figure 7 considering the parameter spaces (b, f), (b, α) and (b, q).

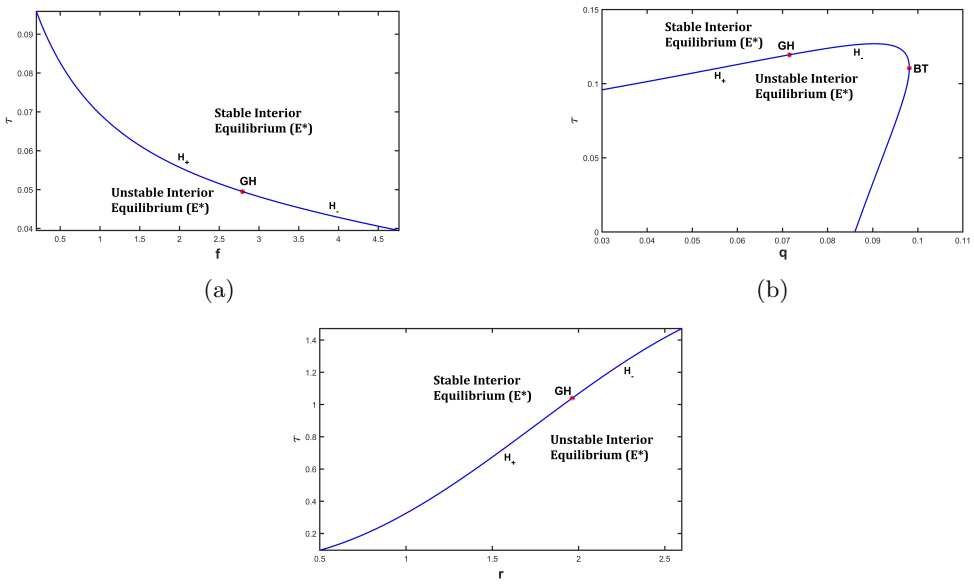

Figure 6: Two-dimensional projection of Hopf bifurcation curves.

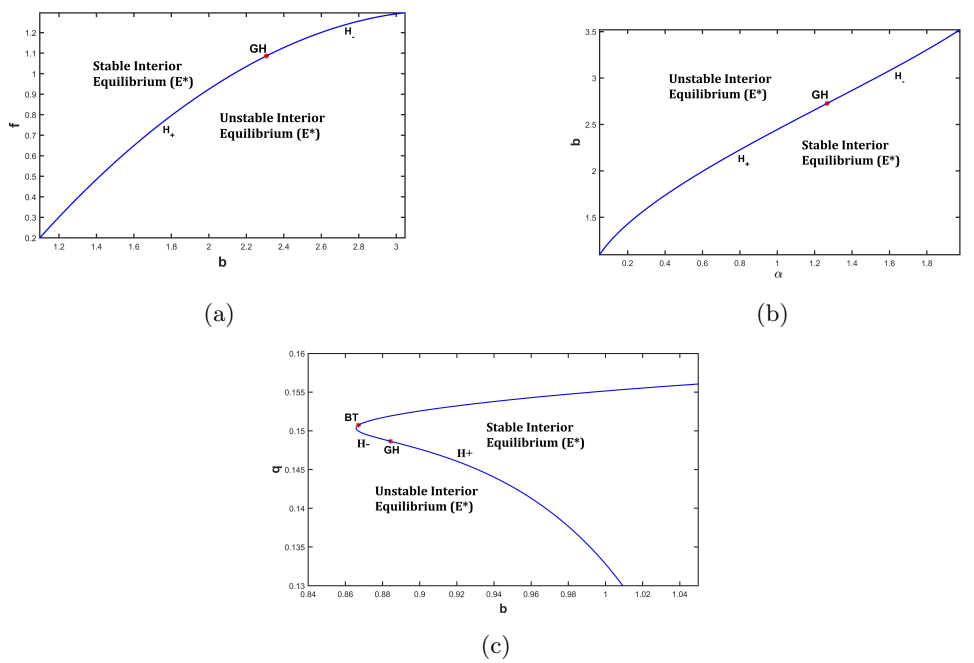

Figure 7: Two-dimensional projection of Hopf bifurcation curves.

Starting from the interior equilibrium E^*, considering b as a free parameter, we plot the curve of interior equilibrium for decreasing values of b. It is observed that the interior equilibrium approaches a prey-free equilibrium at $b = b^{BP} = 0.159919$, where the resulting populations are $S = 0$ and $P = 6.253171$

(Figure 8). For the parameter $b = b^{BP}$, conditions of Theorem 5.1 are satisfied,

$$\begin{aligned} W^T g_b(X, b^{BP})_{E_1} &= 0, \\ W^T Dg_b(X, b^{BP})(V)_{E_1} \frac{\tau w_2 \left(v_1 - 2b^{BP} v_2\right)}{(b^{BP})^2} &= -0.0975063 \neq 0. \\ W^T D^2 g(X, b^{BP})(V, V)_{E_1} - 0.0570662 &\neq 0. \end{aligned}$$

which confirms the validity of the Theorem 5.1. Again for increasing values of α, the interior equilibrium approaches the prey-free equilibrium $E_1 = (0, 2)$ at $\alpha = \alpha^{BP} = 0.549693$ (Figure 9). At this bifurcation point, $W^T D^2 g(X, \alpha^{BP})(V, V)_{E_1} = -0.168253 \neq 0$, satisfying the conditions of Theorem 5.2. Similarly, at $q = q^{BP} = 0.086039$, the interior equilibrium approaches a prey-free equilibrium where the resulting populations are $S = 0$ and $P = 6.253171$ (Figure 10). At this point $W^T D^2 g(X, q^{BP})(V, V)_{E_1} = 0.171847 \neq 0$, fulfilling the conditions of Theorem 5.3. Moreover, the interior equilibrium E^* undergoes a stability exchange with an unstable interior equilibrium through a saddle-node bifurcation at $q^{LP} = 0.098112$. At this bifurcation, the conditions of Theorem 5.4 are satisfied, with $W^T D^2 \hat{h}(X, q^{BP})(V, V)_{E^*} = 2.75006 \neq 0$.

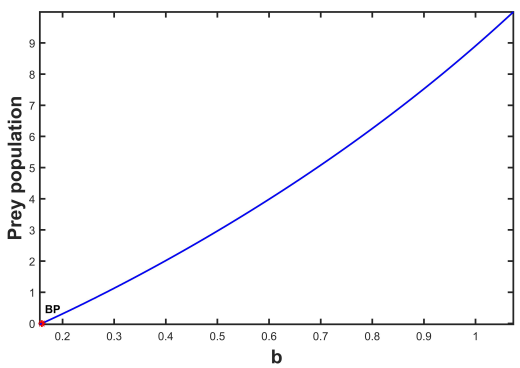

Figure 8: Variation of prey population against b.

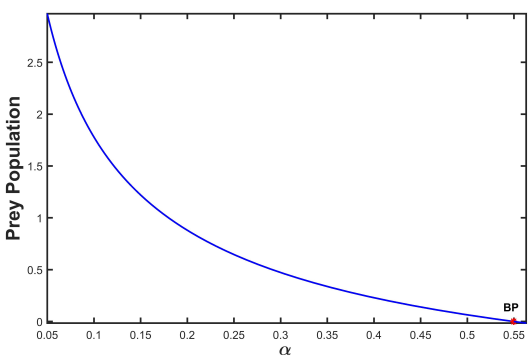

Figure 9: Variation of prey population against α.

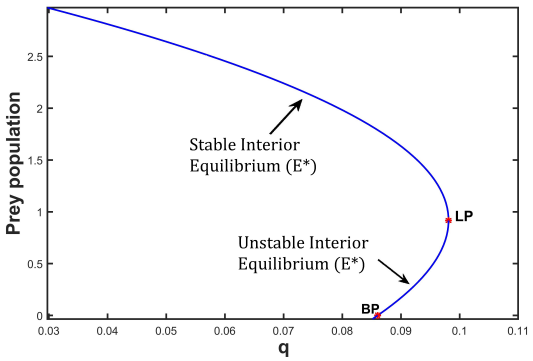

Figure 10: Variation of prey population against q.

7. Results and discussion

Antipredator responses are positively correlated with the intensity of predation pressure, increasing as the number of inducing predators rises. In particular, cooperative hunting strategies adopted by predators during the predation process significantly amplify the fear responses triggered in prey. Motivated by these dynamics, we formulate a new prey–predator model with nonlinear harvesting, explicitly accounting for the fear effects driven by cooperative hunting. To demonstrate the biological feasibility of the model, we examined the positivity and boundedness of the solutions of the proposed mathematical system. Our model admits four biologically meaningful equilibrium points, for which the existence and local stability are thoroughly analyzed. Furthermore, the effects of various parameters on system dynamics are explored both analytically and numerically. Our analysis reveals that when the conversion coefficient b exceeds a critical threshold value b^H, the prey and predator populations display oscillatory behavior, meaning that a stable population state cannot be achieved and fluctuations persist over time. A similar oscillatory pattern is observed when the predator growth rate τ falls below its critical threshold τ^H. Moreover, increasing the catchability coefficient q or the hunting cooperation rate α destabilizes the interior equilibrium, leading to the formation of distinct prey-free equilibrium states. Likewise, a decrease in the conversion coefficient b results in the destabilization of the interior equilibrium, with the system transitioning to a prey-free state. By projecting the Hopf bifurcation curves, we identified regions within the parameter spaces (f, τ), (q, τ), (r, τ), (b, f), (b, α), and (b, q) where the interior equilibrium becomes unstable and the system exhibits periodic oscillations. Additionally, we analyzed the emergence of prey-free states from the interior equilibrium by varying key parameters: the conversion coefficient b, the hunting cooperation rate α, and the catchability coefficient q. The transition from the interior equilibrium to a prey-free state was demonstrated using the Sotomayor theorem, supported by appropriate figures that illustrate the convergence behavior. Our proposed model is novel in its incorporation of both fear effects arising from hunting cooperation and nonlinear harvesting dynamics. In this study, we primarily focused on determining critical threshold parameter values, providing a clear understanding of the model's behavior. In future work, we aim to extend this analysis by investigating optimal harvesting strategies and developing an optimal harvesting policy based on the proposed model.

Acknowledgments

We extend our sincere appreciation to the referees for their thoughtful suggestions that contributed to the improvement of this paper.

Conflict of Interest

The authors affirm that there are no financial or personal connections that could have improperly influenced the content or conclusions presented in this manuscript.

References

1. Alves, M. T., Hilker, F. M., *Hunting cooperation and Allee effects in predators*, J. Theor. Biol, 419, 13-22, (2017).
2. Pal S., Pal, N., Samanta, S., Chattopadhyay, J., *Effect of hunting cooperation and fear in a predator-prey model*, Ecol. Complex., 39, 100770, (2019).
3. Perko, L., *Differential equations and dynamical systems* (Vol. 7), Springer Science & Business Media, (2013).
4. Gese, E. M., Knowlton, F. F., *The role of predation in wildlife population dynamics*, (2001)
5. Glasser, J. W., *The role of predation in shaping and maintaining the structure of communities*, Am. Nat. , 113(5), 631-641, (1979).
6. Solomon, M. E., *The natural control of animal populations*, The Journal of Animal Ecology, 1-35, (1949).
7. Cresswell, W., *Predation in bird populations*, J. Ornithol., 152(Suppl 1), 251-263,(2011).
8. Lima Steven L., *Nonlethal effects in the ecology of predator-prey interactions*, Bioscience, 48(1): 25-34, (1998)
9. Peacor Scott D., Pangle, K. L., Schiesari, L., Earl E., *Scaling-up anti-predator phenotypic responses of prey: impacts over multiple generations in a complex aquatic community*, Proc. R. Soc. Lond., 279(1726), 122-128, (2012).
10. Clinchy M., Sheriff M. J., Zanette L. Y., *Predator-induced stress and the ecology of fear*, Funct. Ecol., 27(1), 56-65, 2013.
11. Kashyap, A. J., Sarmah, H. K., Bhattacharjee, D., *An eco-epidemiological model with non-consumptive predation risk and fatal disease in prey*, Journal of Mathematical Sciences, 1-31, (2024).
12. Zanette, L.Y., White, A.F., Allen, M.C., Clinchy, M.,*Perceived predation risk reduces the number of offspring songbirds produce per year*, Science 334(6061), 1398–1401 (2011)
13. Kashyap, A. J., Sarmah, H. K., *Complex Dynamics in a Predator–Prey Model with Fear Affected Transmission*, Differ. Equ. Dyn. Syst., 1-32, (2024).
14. Kashyap, A. J., Bhattacharjee, D., Sarmah, H. K., *A fractional model in exploring the role of fear in mass mortality of pelicans in the Salton Sea*, An International Journal of Optimization and Control: Theories & Applications (IJOCTA), 11(3), 28-51, (2021).
15. Stander, P.E., *Cooperative hunting in lions: the role of the individual*, Behav. Ecol. Sociobiol, 29, 445–54, (1992).
16. Ripple, W.J., Larsen, E.J., *Historic aspen recruitment, elk, and wolves in northern Yellowstone National Park, USA* Biol. Conserv. 95, 361–70 (2000).
17. Uetz, G.W., *Foraging strategies of spiders*, Trends Ecol. Evol. 7, 155–159 (1992)
18. Boesch, C., Boesch, H., Vigilant, L., In Kappeler, P.M., Van Schaik, C.P. (eds), *Cooperation in Primates and Humans: Mechanisms of Evolution*, 4–21. Springer, New York, (2006).
19. Feh, C., Boldsukh, T., Tourenq, C., *Are family groups in equids a response to cooperative hunting by predators ? The case of Mongolian kulans (Equus hemionus luteus Matschie)*, Rev. Ecol. 49, 11–20, (1994)
20. Schmidt, P.A., Mech, L.D., *Wolf pack size and food acquisition*, Am. Nat., 150(4), 513–517 (1997).
21. Creel, S., Winnie, J.A., Jr., *Responses of elk herd size to fine-scale spatial and temporal variation in the risk of predation by wolves* Anim. Behav. 69(5), 1181–1189 (2005).
22. Creel, S., Winnie, J.A., Jr., Maxwell, B., Hamlin, K., Creel, M., *Elk alter habitat selection as an anti-predator response to wolves*, Ecology, 86(12), 3387–3397, (2005).
23. Gupta R. P., Chandra P., *Bifurcation analysis of modified leslie-gower predator-prey model with Michaelis-Menten type prey harvesting*, J. Math. Anal. Appl., 398, 278–295, (2013).
24. Kashyap A. J., Zhu, Q., Sarmah, H. K., Bhattacharjee, D., *Dynamical study of a predator-prey system with Michaelis-Menten type predator-harvesting*, Int. J. Biomath., 16(8), 2250135, (2023).

Mustak Euchuf,

The Assam Royal Global University, Guwahati, 781035, India.

E-mail address: mustak.euchuf.1234@gmail.com

and

Ankur Jyoti Kashyap,

Girijananda Chowdhury University, Guwahati, 781017, India.

E-mail address: ajkashyap.maths@gmail.com

and

Anuradha Devi,
The Assam Royal Global University, Guwahati, 781035, India.
E-mail address: anuradha.devi@rgi.edu.in